Available online at www.sciencedirect.com
SCIENCE DIRECT
Journal of Photochemistry and Photobiology A: Chemistry 177 (2006) 286–294
Journal of Photochemistry and Photobiology A:Chemistry
www.elsevier.com/locate/jphotochem

Aryl-modified ruthenium bis(terpyridine) complexes: Quantum yield of $^1O_2$ generation and photocleavage on DNA

Hui-Ying Ding [a,b], Xue-Song Wang [a,*], Lin-Qing Song [a], Jing-Rong Chen [a], Jun-Hua Yu [a], Chao-Li [a,b], Bao-Wen Zhang [a,*]

[a] *Technical Institute of Physics and Chemistry Chinese Academy of Sciences Beijing, PR China*
[b] *Graduate School of the Chinese Academy of Sciences, Beijing 100039, PR China*

Received 30 January 2005; received in revised form 30 April 2005; accepted 7 June 2005
Available online 15 July 2005

Abstract

Six Ru(II)bis(tpy) (tpy = 2,2′:6′,2″-terpyridine) complexes, functionalized with one or two 2-naphthyl, 1-pyrenyl, or 9-anthracenyl at 4′-position of terpyridine respectively, were investigated with emphasis on their $^1O_2$ generation quantum yields and photocleavage capabilities on DNA. For naphthyl and pyrenyl modified complexes, the lowest energy excited state is ^{3}MLCT, and therefore they behave very similarly to the parent complex, $[Ru(tpy)_2]^{2+}$, having very low $^1O_2$ generation quantum yields. In contrast, for anthracenyl modified complexes, the lowest energy excited state is anthracene-localized $^3\pi\pi^*$ state, as a result, they exhibit extremely high $^1O_2$ generation quantum yields (0.96 and 0.71 for bis- and mono-substituted complexes, respectively) and potent photodamage abilities on calf thymus DNA, suggesting their promising applications in $^1O_2$-involved processes, such as DNA photocleavage.

Keywords: Calf thymus DNA; Photocleave; Ruthenium; Singlet oxygen

1. Introduction

By virtue of their rich photophysical, photochemical, and redox properties as well as their unusual binding capabilities on DNA, ruthenium(II) polypyridyl complexes have received extensive studies as DNA site-specific or conformation-specific markers and photo cleavers [1]. In photocleavages of DNA activated by Ru(II) polypyridyl complexes, where no direct chemical reactions (such as electron transfer and oxo transfer) occurred between the complexes and DNA, singlet oxygen ($^1O_2$) generated via energy transfer from triplet metal-to-ligand charge transfer states (^{3}MLCT) of the complexes is believed to initiate the strand breaks [2–4]. As a result, the photocleavage efficiencies of Ru(II) complexes depend generally on their $^1O_2$ generation ability and their binding strength upon DNA.

A variety of Ru(II) tris(bidentate) complexes, e.g. tris-bipyridyl, trisphenanthroline Ru(II) complexes or their substituted analogues, can effectively photoactivate cleavage of DNA [2–4], because they can generate $^1O_2$ efficiently benefited mainly by their long lifetimes of ^{3}MLCT (in μs region) [5–8], and because they can associate with DNA strongly by way of intercalative diimine ligands such as dipyrido[3,2-a:2′,3′-c]phenazine (dppz)[1]. In contrast, no Ru(II) bis(terdentate) complexes were used as DNA photocleavage agent due to their poor $^1O_2$ generation ability, which in turn results predominantly from their very short lifetimes of ^{3}MLCT (in ns region) [9].

Compared to Ru(II) tris(bidentate) complexes, Ru(II) bis(terdentate) complexes exhibit many advantages. For example, $[Ru(bpy)_3]^{2+}$ (bpy = 2,2′-bipyridine) exists in two enantiomeric forms which may complicate its interaction with DNA, while $[Ru(tpy)_2]^{2+}$ (tpy = 2,2′:6′,2″-terpyridine) is achiral [10]. Also, rod-like superamolecular systems based on $[Ru(bpy)_3]^{2+}$, in which vectorial energy and electron

* Corresponding authors. Tel.: +86 10 64888103; fax: +86 10 64879375.
E-mail address: g203@mail.ipc.ac.cn (B.-W. Zhang).

1010-6030/$ – see front matter © 2005 Elsevier B.V. All rights reserved.
doi:10.1016/j.jphotochem.2005.06.008

transfer is favored, are difficult to construct, while such structures made from $[Ru(tpy)_2]^{2+}$ are fully developed [9,11–13]. Therefore, many strategies have been applied to improve the photophysical properties of Ru(II) bis(terdentate) complexes, including the utilization of cyclometalating ligands [9], the incorporation of electron donating or withdrawing substituents in terdentate ligands [14], and increasing the delocalization ability of the terdentate ligands [15]. Recently another approach, namely "reservoir effect" which first demonstrated its potent ability to increase the ^{3}MLCT lifetimes of Ru(II) tris(diimine) complexes [16,17], was successfully adopted to lengthen the ^{3}MLCT lifetimes of Ru(II) bis(terpyridine) complexes greatly [18–20]. The underlying mechanism is the establishment of a fast equilibration between the ^{3}MLCT state of the complex and the triplet excited state of the attached organic chromophore on ligand which is very longlived and locates close to ^{3}MLCT in energy. Thus, excitation in ^{1}MLCT band of the Ru(II) complex results in the population of the triplet excited state of the organic chromophore, which then serves as an energy reservoir to allow the ^{3}MLCT relax in a much longer time domain through the equilibration mentioned above.

Organic chromophores used in this regard are generally pyrene and anthracene due to the proper energies of their triplet excited states. Taking it in mind that $^1O_2$ can be effectively generated via energy transfer from the triplet excited states of pyrene and anthracene, the presence of these aryl chromophores may provide an efficient channel to generate $^1O_2$ via excitation of ^{1}MLCT of the Ru(II) complex moiety. For example, $^1O_2$ was generated efficiently via triplet excited states of pyrenyl groups attached directly on phenanthroline ligands in $[Ru(py\text{-}phen)_3]^{2+}$ [21]. This is probably of more importance for Ru(II) bis(terpyridine) complexes because of their poor $^1O_2$ generation ability. Moreover, aryl units are also known to be efficient intercalators, and naphthalene, anthracene, and pyrene modified Ru(II) bis(terpyridine) complexes have proved to bind calf thymus DNA (CT-DNA) strongly by intercalation interaction of these aryl substituents [10]. These facts suggest that modification of $[Ru(tpy)_2]^{2+}$ with aryl chromophores may afford a new type of DNA photocleavers.

In this contribution the $^1O_2$ generation abilities of $[Ru(tpy)_2]^{2+}$ and its six derivatives substituted by one or two 2-naphthyl, 1-pyrenyl, and 9-anthracenyl in the 4′-position of the terpyridine ligands (see Scheme 1 for them and corresponding ligands) were investigated and their photodamages on CT-DNA were also examined. Although $^1O_2$ formation was observed in an anthracenyl-modified Ru(II) bis(terpyridine) complex [22], more concerns were focused on the ^{3}MLCT lifetime tuning abilities of the introduced aryl units [18–20]. To the best of our knowledge, this is the first case in which the effects of substituted aryl groups on the $^1O_2$ generation and photodamage to DNA were emphasized for Ru(II) complexes of terpyridine-type ligands.

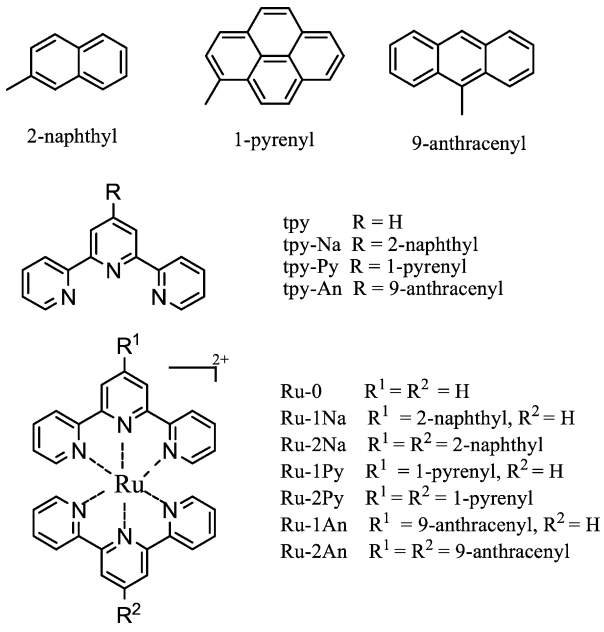

Scheme 1. Chemical structures of aryl-substituted terpyridine ligands and their Ru(II) complexes.

2. Experimental

2.1. Materials

2,2,6,6-Tetramethyl piperidine (TEMP), ethidium bromide (EB), 1,3-diphenylisobenzofuran (DPBF), 2,2′-bipyridine (bpy), 2,2′:6′,2″-terpyridine (tpy), 2-acetylpyridine, 9-anthraldehyde, 1-pyrenecarboxaldehyde, 2-naphthaldehyde were purchased from Aldrich and used as received. Calf thymus DNA (CT-DNA) was obtained from Sigma Chemical Company. The concentration of CT-DNA is expressed as the concentration of nucleotide and was determined using the extinction coefficient of $6600\,M^{-1}\,cm^{-1}$ at 260 nm. Solvents used in spectrum measurements were purified following general procedures [23]. Ligand tpy-Na, tpy-Py, and tpy-An were prepared with reported methods [24]. $[Ru(tpy)_2]$ $(PF_6)_2$ and $[Ru(bpy)_3](PF_6)_2$ were synthesized following literature approaches [25,26].

2.1.1. Synthesis of aryl-substituted Ru(II) bis (terpyridine) complexes

Mono-substituted Ru(II) bis(terpyridine) complexes: Tpy-An (84 mg, 0.2 mmol) and triethylamine (50 μL) were successively added to a suspension of $Ru(tpy)Cl_3$ [27] (90 mg, 0.2 mmol) in *n*-butyl alcohol (20 mL) and refluxed for 12 h in the dark and Ar atmosphere. After cooling, an excess of aqueous ammonium hexafluorophosphate was added to precipitate crude $(Ru\text{-}lAn)(PF_6)_2$. Pure product was obtained by chromatography over Al_2O_3 using dichloromethane–acetonitrile–methanol (10:1:1 in volume ratio) containing 1% triethylamine as eluent. Hexafluorophosphate salts of Ru-1Na and Ru-1Py were prepared in a similar way.

(Ru-lNa)$(PF_6)_2$ yield 77 mg (39%). ^{1}H NMR (300 MHz, d_6-acetone): δ 9.59 (s, 2H), 9.09 (d, J = 8.1 Hz, 2H), 9.07 (d, J = 8.1 Hz, 2H), 8.90 (s, 1H), 8.82 (d, J = 8.1 Hz, 2H), 8.59 (t, J = 8.1 Hz, 1H), 8.43 (d, J = 8.4 Hz, 1H), 8.28 (d, J = 8.4 Hz, 1H), 8.05–8.17 (m, 4H), 7.84 (d, J = 5.4 Hz, 2H), 7.73 (d, J = 5.4 Hz, 2H), 7.69 (m, 2H), 7.34 (m, 4H). MALDI-TOF MS: m/z 694.0 $(M\text{-}2PF_6)^+$. Anal. Calcd for $C_{40}H_{28}N_6P_2F_{12}Ru{\cdot}2H_2O$: C, 47.11; H, 3.16; N, 8.24. Found: C, 47.08; H, 3.00; N, 8.00.

(Ru-lPy)$(PF_6)_2$ yield 89 mg (42%). ^{1}H NMR (300 MHz, d_6-acetone): δ 9.42 (s, 2H), 9.24 (d, J = 8.1 Hz, 2H), 9.05 (d, J = 8.1 Hz, 2H), 8.85 (d, J = 8.1 Hz, 2H), 8.35–8.71 (m, 9H), 8.21 (t, 1H, J = 7.5 Hz), 8.15 (dd, J = 8.1 Hz, 5.4 Hz, 2H), 8.09 (dd, J = 8.1 Hz, 5.4 Hz, 2H), 7.95 (d, J = 5.4 Hz, 2H), 7.80 (d, J = 5.4 Hz, 2H), 7.78 (m, 4H). MALDI-TOF MS: m/z 766.6 $(M\text{-}2PF_6)^+$. Anal. Calcd for $C_{46}H_{30}N_6P_2F_{12}Ru{\cdot}2.5H_2O$: C, 50.10; H, 3.20; N, 7.62. Found: C, 49.86; H, 3.06; N, 7.65.

(Ru-lAn)$(PF_6)_2$ yield 83 mg (40%). ^{1}H NMR (300 MHz, d_6-acetone): δ 9.20 (s, 2H), 9.12 (d, 2H, J = 8.1 Hz), 8.93 (s, 1H), 8.92 (d, 2H, J = 7.8 Hz), 8.86 (d, 2H, J = 8.4 Hz), 8.61 (t, 1H, J = 8.1 Hz), 8.32 (d, 2H, J = 8.4 Hz), 8.0–8.2 (m, 8H), 7.78 (d, 2H, J = 8.1 Hz), 7.67 (dd, 2H, J = 7.2 Hz, 7.8 Hz), 7.57 (dd, 2H, J = 7.2 Hz, 8.4 Hz), 7.42 (dd, 2H, J = 6.3 Hz, 8.1 Hz), 7.35 (dd, 2H, J = 6.0 Hz, 6.3 Hz). MALDI-TOF MS: m/z 742.8 $(M\text{-}2PF_6)^+$, 887.8 $(M\text{-}PF_6)^+$. Anal. Calcd for $C_{44}H_{30}N_6F_2P_{12}Ru{\cdot}2.5H_2O$: C, 48.99; H, 3.27; N, 7.79. Found: C, 49.11; H, 3.01; N, 7.73.

Bis-substituted Ru(II) bis(terpyridine) complexes. Tpy-An (168 mg, 0.4 mmol) and triethylamine (50 μL) were successively added to a suspension of $Ru(DMSO)_4Cl_2$ [27] (49 mg, 0.2 mmol) in *n*-butyl alcohol (20 mL) and refluxed for 24 h in the dark and Ar atmosphere. Work up as mentioned above gave (Ru-2An)$(PF_6)_2$. (Ru-2Na)$(PF_6)_2$ and (Ru-2Py)$(PF_6)_2$ were prepared similarly.

(Ru-2Na)$(PF_6)_2$ yield 100 mg (45%). ^{1}H NMR (300 MHz, d_6-acetone): δ 9.60 (s, 4H), 9.10 (d, J = 7.8 Hz, 4H), 8.93 (s, 2H), 8.47 (d, J = 8.4, 2H), 8.29 (d, J = 8.4 Hz, 2H) 8.19–8.12 (m, 8H), 7.87 (d, J = 6.0 Hz,4H), 7.71 (m, 4H), 7.37 (dd, J = 6.0 Hz, 6.6 Hz, 4H). MALDI-TOF MS: m/z 818.9 $(M\text{-}2PF_6)^+$. Anal. Calcd for $C_{50}H_{34}N_6P_2F_{12}{\cdot}3H_2O$: C, 51.59; H, 3.43; N, 7.22. Found: C, 51.75; H, 3.21; N, 7.29.

(Ru-2Py)$(PF_6)_2$ yield 116 mg (46%).^{1}H NMR (300 MHz, d_6-acetone): δ 9.50 (s, 4H), 9.11 (d, J = 8.1 Hz, 4H),9.78 (d, J = 9.0 Hz, 2H), 8.69 (d, J = 7.9 Hz, 2H), 8.52 (m, 12H), 8.27 (t, J = 7.5 Hz, 2H), 8.19 (dd, J = 7.2 Hz, 8.1 Hz, 4H), 8.09 (d, J = 5.4 Hz, 4H), 7.49 (dd, J = 5.4 Hz, 7.2 Hz, 4H). MALDI-TOF MS: m/z 967.0 $(M\text{-}2PF_6)^+$. Anal. Calcd for $C_{62}H_{38}N_6P_2F_{12}Ru{\cdot}2H_2O$: C, 57.55; H, 3.27; N, 6.49. Found: C, 57.56; H, 3.28; N, 6.44.

(Ru-2An)$(PF_6)_2$ yield 116 mg (48%). ^{1}H NMR (300 MHz, d_6-acetone): δ 9.25 (s, 4H), 8.97 (d, J = 7.8 Hz, 4H), 8.95 (s, 2H), 8.34 (d, J = 8.4 Hz, 4H), 8.20–8.00 (m, 12H), 7.69 (dd, J = 8.4 Hz, 6.6 Hz, 4H), 7.59 (dd, J = 7.8 Hz, 6.6 Hz, 4H), 7.46 (dd, J = 6.6 Hz, 6.3 Hz, 4H). MALDI-TOF MS: m/z 918.6 $(M\text{-}2PF_6)^+$. Anal. Calcd for $C_{58}H_{38}N_6P_2F_{12}Ru{\cdot}2.5H_2O$: C, 55.51; H, 3.45; N, 6.70. Found: C, 55.24; H, 3.17; N, 6.82.

2.2. Transient absorption spectrum measurements

Nanosecond time-resolved absorption spectroscopy was performed using the second harmonic (532 nm, 5 ns fwhm) output of a Nd:YAG laser for excitation, a pulsed flashlamp (Xe 900) for the analyzing light and PMT (Edinburgh Instruments LP920) for the transient detection.

2.3. ESR measurements

The ESR spectra were recorded at room temperature (25 °C) on a Bruker ESP-300E spectrometer at 9.8 GHz, X-band with 100 Hz field modulation. Samples were injected quantitatively into specially made quartz capillaries for ESR analysis, and purged with argon or oxygen for 30 min in the dark respectively, according to the experimental requirement and illuminated directly in the cavity of the ESR spectrometer with a Nd:YAG laser at 532 nm (5–6 ns of pulse width, 10 Hz of repetition frequency, 30 mJ/pulse energy) or 355 nm (5–6 ns of pulse width, 10 Hz of repetition frequency, 10 mJ/puse energy). $^1O_2$ was detected by using TEMP as spin trap.

2.4. Quantum yield of $^1O_2$ generation

The reaction of $^1O_2$ with 1,3-diphenylisobenzofuran [28] (DPBF, Scheme 2) was adopted to measure the quantum yields of $^1O_2$ generation for Ru(II) bis(terpyridine) complexes.

A series of 2 mL of air-saturated methanol solutions containing DPBF (20 μM) and complexes, of which the absorbance at 480 nm originating from the absorption of complexes was adjusted to the same ($OD_{480\,nm}$ = 0.08), were separately charged into an opened 1 cm path fluorescence cuvette and illuminated with light of 480 nm (obtained from a Hitachi F-4500 fluorescence spectrophotometer, 10 nm of excitation slit width). The consumptions of DPBF were followed by monitoring its fluorescence intensity decrease at the emission maximum (λ_{ex} = 405 nm, λ_{em}^{max} = 479 nm) at different irradiation time. $[Ru(bpy)_3]^{2+}$ was used as standard, whose $^1O_2$ generation quantum yield was determined to be 0.81 in air saturated methanol [6].

2.5. Ethidium bromide assay for DNA cleavage

An air-saturated EB/CT-DNA buffer solution (5 mM ammonium acetate, 50 mM sodium chloride, pH 7, 80 μM EB, 40 μM CT-DNA) containing a Ru(II) complex (2 μM or 2.5 μM) was irradiated in a 'merry go round' apparatus with

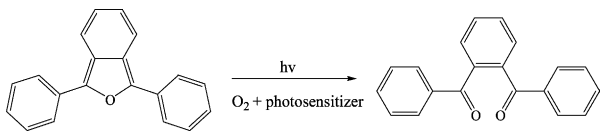

Scheme 2. The reaction of DPBF with singlet oxygen.

a medium pressure mercury lamp (light below 470 nm was cut off by a glass filter). The cleavage of CT-DNA was examined by measuring fluorescence emission spectrum from 525 to 800 nm (λ_{ex} = 510 nm) at variant irradiation time.

3. Results and discussion

3.1. Photophysical properties of Ru(II) bis(terpyridine) complexes

Shown in Fig. 1 are the UV–vis absorption spectra of the six aryl-modified Ru(II) bis(terpyridine) complexes along with their parent complex $[Ru(tpy)_2]^{2+}$ (Ru-0) in acetonitrile. All of them show typical MLCT bands in the visible region (Table 1). The substitutions of aryl groups at the 4′-position of terpyridine ligands give rise to small red shifts of the MLCT absorption maxima with respect to Ru-0. Though 2-naphthyl and 1-pyrenyl differ distinctively in their properties, particularly in the sizes of their π-conjugation systems, the red shift effects they exhibit are the same, suggesting a non-planar orientation between terpyridine and 2-naphthyl or 1-pyrenyl. Also, the red shift ability of 9-anthracenyl is the weakest among the aryl groups used, implying a more twisted conformation between terpyridine and 9-anthracenyl. This assumption is consistent with the reported crystal structures of tpy-Py, tpy-An, and their corresponding Ru(II) complexes [24]. Single crystal X-ray diffraction indicate that the angle between the pyrenyl ring in tpy-Py and the plane of the central pyridyl ring of the terpyridine moiety is 51.6°, while the corresponding angle is 74.5° in tpy-An [24]. Such twisted conformations are remained in crystals of their Ru(II) complexes. Large deviation from the coplanarity arises largely from the tendency of either molecule to adopt the conformation of the lowest energy by avoiding the non-bonded contacts between the H atoms at 1- and 8-positions of the anthryl ring, or H atom at 10-position of the pyrenyl ring and those of the central pyridyl ring (3′-H and 5′-H) respectively [24].

The highly twisted orientations of aryl substituents relative to terpyridine moiety lead to weak electronic interactions of these periphery aryls and $[Ru(tpy)_2]^{2+}$ core. This is most clearly illustrated in Ru-1An and Ru-2An, where the absorption features attributed to anthracene can be resolved in the

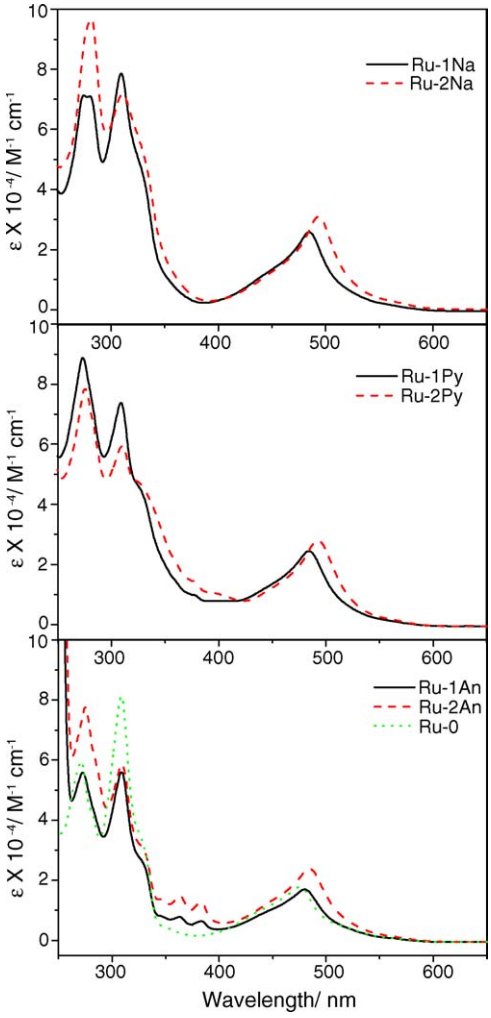

Fig. 1. Adsorption spectra of the aryl-modified. Ru(II) bis(terpyridine) complexes in CH_3CN at room temperature.

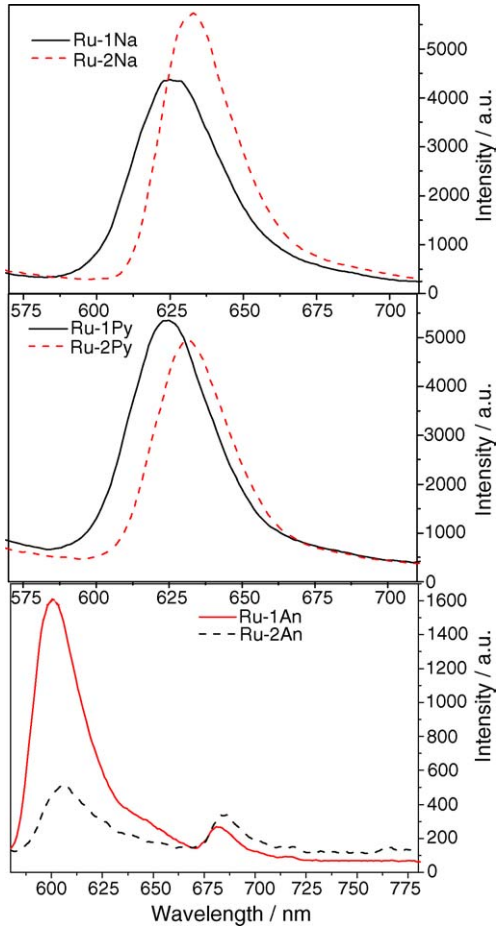

Fig. 2. Emission spectra of the aryl-moditied Ru(II) bis(terpyndme)-complexes in ethanol/methanol (4:1) glass matrix at 77 K.

Table 1
Photophysical properties of Ru(II) bis(terpyridine) complexes

	Ru-0	Ru-1Na	Ru-2Na	Ru-1Py	Ru-2Py	Ru-1An	Ru-2An
λ_{max}^{ab} [a] (nm)	476	484	493	484	491	480	483
λ_{max}^{em} [b] (nm)	597	625	633	626	632	600, 684[c]	606, 684[c]
Φ_{Δ} [d]	0.016	0.016	0.016	0.029	0.073	0.71	0.96

[a] Absorption maximum of MLCT band in CH_3CN.
[b] Emission maximum in ethanol/methanol (4:1 in volume ratio) glass matrix at 77 K.
[c] Dual emission.
[d] Measured in air-saturated methanol solutions using $[Ru(bpy)_3]^{2+}$ as standard.

region from 350 to 400 nm (Fig. 1). The weak electronic interactions warrant a localized description of aryl-substituted $[Ru(tpy)_2]^{+}$ as shown in Scheme 2, with energy level diagrams obtained as a superposition of those of $[Ru(tpy)_2]^{2+}$ core and aryl peripheries. The most energy levels drawn in Scheme 3 are based on the related data from Refs. [9] and [16], respectively, except that the energy of ^{1}MLCT of Ru-0 is estimated from its absorption onset at about 540 nm.

At room temperature all complexes studied are nonluminescent even in the absence of O_2 (dissolved O_2 was removed by freeze-pump-thaw cycles), irrespective of the excitation wavelengths (250–550 nm). This result is not surprising as far as the energy levels involved are considered. For Ru-1Na, Ru-2Na, Ru-1Py and Ru-2Py, excitation both upon allowed transitions of ^{1}MLCT or ^{1}LC (ligand-centered state, not shown in Scheme 3) of $[Ru(tpy)_2]^{2+}$ moiety and $^1\pi\pi^*$ of aryl groups will eventually results in the population of ^{3}MLCT, followed by radiationless decay via an upper lying triplet metal-centered state (^{3}MC, not shown in Scheme 3) as their parent complex Ru-0 [9]. In the cases of Ru-1An and Ru-2An, the lowest excited state of ^{3}An is a nonemissive state at room temperature, as a result no emission was detected.

At 77 K luminescence with maxima at 625, 633, 626, and 632 nm for Ru-1Na, Ru-2Na, Ru-1Py and Ru-2Py, respectively were observed (Fig. 2 and Table 1), which can be ascribed to the ^{3}MLCT emission, consisting with the assumption that the lowest energy excited states in these complexes are ^{3}MLCT states. The significant red shifts in emission as large as 36 nm with respect to the parent complex Ru-0 (597 nm) implies the electronic interactions between

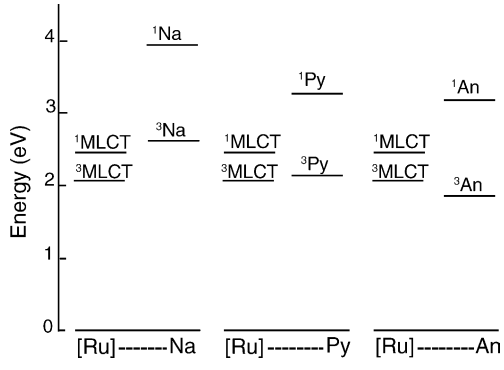

Scheme 3. Energy level diagrams for aryl-substituted $[Ru(tpy)_2]^{2+}$ complexes.

$[Ru(tpy)_2]^{2+}$ moiety and naphthyl or pyrenyl group increase to some extent in the excited state. In contrast, dual emission was observed for Ru-1An and Ru-2An (Fig. 2) though the luminescence intensities for them are much lower than naphthyl- or pyrenyl-substituted complexes. The luminescence centered at about 684 nm for both Ru-1An and Ru-2An can be attributed to the anthracene triplet by referring to the reported results [18,32,33], while the luminescence at 600 nm for Ru-1An and 606 nm for Ru-2An is likely of ^{3}MLCT origin due to the similarity to the emission of Ru-0 at 77 K. The dual emission may result from the inefficient quenching of ^{3}MLCT by ^{3}An, which seems to be in line with the observation that the intensity ratio of the short wavelength emission with the long one in Ru-1An is much higher than that in Ru-2An. Ru-0 may be present as luminescent impurity in Ru-1An solution and account for the emission at 600 nm, though the emission maximum of Ru-0 (597 nm) was found to be somewhat blue shifted. However, it is not possible that Ru-0 was present in Ru-2An solution because no tpy ligand was used in the synthesis of Ru-2An, suggesting that Ru-0 alone, if any, cannot account for the emission bands at 600 nm for Ru-1An and 606 nm for Ru-2An. Also, further purification did not change the relative intensity of two emission bands for both Ru-1An and Ru-2An. Moreover, excitation spectra indicated that both emissions came from MLCT absorption bands of Ru-1An and Ru-2An, ruling out luminescent impurities as the origin of the dual emission further.

Time-resolved absorption spectroscopy was also applied to study the excited state properties of these Ru complexes. Up to the upper time limit of the instrument, no transient absorptions were detected for Ru-1Na, Ru-2Na, Ru-1Py, Ru-2Py, and Ru-0, in good agreement with that the lowest energy excited states in them are of ^{3}MLCT origin, and therefore short-lived. In contrast, transient absorption spectra of Ru-1An and Ru-2An were recorded readily as shown in Fig. 3 (Ru-1An and Ru-2An behaved very similarly). The negative absorption band between 350 and 380 nm and the very strong positive absorption centered at 420 nm can be attributed to the ground state bleaching of An groups and triplet–triplet transition of ^{3}An respectively, indicating the population of ^{3}An upon excitation of MLCT band. Similar transient absorptions were observed in $[(bpy)(CO)C1Os(bpy\text{-}An)]^{+}$ [16] and $[Ru(bpy)_2(bpy\text{-}CH_2CH_2\text{-}An)]^{2+}$ [32], where triplet excited state localized in An group is the lowest energy excited state. Interestingly, a negative absorption centered at 480 nm and a

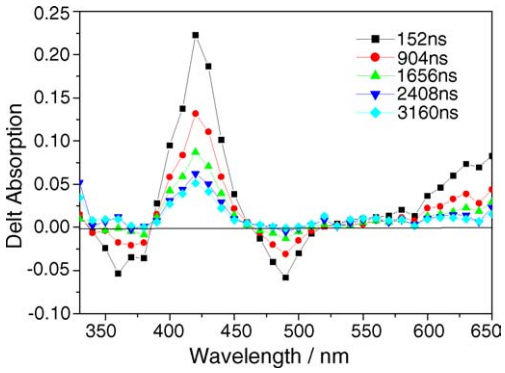

Fig. 3. Time-resolved absorption spectra of Ru-2An in degassed methanol solution after pulsed excitation at 532 nm.

weak but monotonously intensified positive absorption with increasing wavelength above 550 nm were also observed, and tentatively ascribed to the bleaching of MLCT band and excited state absorption of ^{3}MLCT by comparison with the ground state absorption of Ru-2An and transient absorption spectrum of [Ru(tpy)(tpy-Py)] $^+$[19], in which a gradually increased absorption band with increasing wavelength in the range of 550–700 nm was assigned to the triplet–triplet transition of ^{3}MLCT [19]. The co-existence of the transient absorption bands with ^{3}An and ^{3}MLCT characters respectively, on one hand, implies ^{3}An may serve as the energy reservoir, and as a result lengthen the lifetime of ^{3}MLCT greatly (973 ns by monitoring the bleaching recovery at 480 nm). On the other hand, the comparable partitioning of excited state on both ^{3}An and ^{3}MLCT, deduced from the intensity of two bleaching bands, indicates the inter-conversion between ^{3}An and ^{3}MLCT is not equilibrated, otherwise the ^{3}An will dominate transient absorption because ^{3}An locates about 1800 cm^{-1} below ^{3}MLCT (Scheme 3). It is estimated 99.98% of the excited state would localize on ^{3}An provided the transition between ^{3}An and ^{3}MLCT is equilibrated (the free energy change of the equilibrium $\Delta G = -1800\ \text{cm}^{-1}$, and therefore the equilibrium constant $K_{eq} = 5558$). The co-existence of ^{3}An and MLCT agrees well with the dual emission observation at 77 K.The perpendicular orientation of An moiety with respect to terpyridine ligand might play somewhat role in the non-equilibrated inter-conversion of ^{3}An and ^{3}MLCT. Moreover, a slightly larger energy gap (1800 cm^{-1}) may also disfavor the energy transfer from ^{3}MLCT to ^{3}An as observed in a series of Re(I) complexes linked to anthracene where larger energy transfer driving force corresponded to lower transfer rate [34]. These findings suggest it is worth to carry out ultrafast transient absorption measurements (in ps or even fs domain) for getting into the insight of the interaction of ^{3}An with ^{3}MLCT. ^{3}An in Ru-1An and Ru-2An both decayed, monitored at 425 nm in degassed methanol solutions, mono-exponentially with lifetime of 1314 and 1570 ns, respectively.

The steady-state emission spectra and time-resolved absorption spectra confirmed the population of ^{3}An in Ru-1An or Ru-2An upon excitation of ^{1}MLCT of $[Ru(tpy)_2]^{2+}$ unit, which in turn may provide an efficient pathway to generate $^1O_2$ if O_2 is present.

3.2. $^1O_2$ generation abilities of Ru(II) bis (terpyridine) complexes

Spin trapping is a powerful technique to detect the formation of reactive oxygen, and in our experiments 2,2,6,6-tetramethyl piperidine (TEMP) was used as $^1O_2$ trapping agent to evaluate qualitatively the $^1O_2$ generation abilities of the ruthenium complexes examined. Upon irradiation of oxygen-saturated DMSO solutions of Ru(II) complexes with pulsed laser at 532 or 355 nm, a three-line ESR signal was observed with the hyperfine splitting constant of 16.0 G and g factor of 2.0056 (inset of Fig. 4), in good agreement with TEMPO (the adduct of TEMP and $^1O_2$) signal [35]. Control experiments indicate that the O_2, light, and Ru(II) complexes are all essential to the generation of ESR signals. The addition of 1,4-diazabicyclo[2,2,2] octane (DABCO), an effective scavenger of $^1O_2$, quenched the ESR signal remarkably. All these findings indicate the Ru(II) bis(terpyridine) complexes can generate $^1O_2$ photochemically, and among them Ru-2An and Ru-1An exhibit much higher efficiencies (at least one order of magnitude higher) to generate $^1O_2$ than the others (Figs. 4 and 5). The most significant difference of Ru-2An or Ru-1An from other complexes is that the lowest energy excited state is ^{3}An rather than ^{3}MLCT, from which $^1O_2$ can be produced efficiently. When irradiation was carried out at 355 nm, the $^1O_2$ generation abilities of anthracenyl substituted Ru(II)complexes and anthracene itself, whose $^1O_2$ generation quantum yield was measured to be 0.6 1 [36], can be compared directly. It was found that Ru-2An can generate $^1O_2$ even more efficiently than anthracene, suggesting the efficient intersystem crossing of MLCT states of the $[Ru(tpy)_2]^{2+}$ core may enhance the quantum yield for the population of ^{3}An, which obviously results from

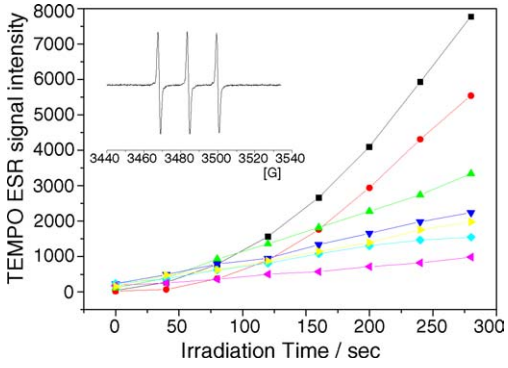

Fig. 4. Dependence of TEMPO signal intensity on the irradiation time in oxygen—saturated DMSO solutions of TEMP (10 μM) and ruthenium complexes (o.d. = 0.17 at 532 nm). The receiver gains for Ru-2An (■) and Ru-lAn (●) were 1×10^4, while for Ru-2Py (▲), Ru-lPy (▼), Ru-2Na (♦), Ru-lNa (◄) and Ru-0 (►) 1×10^5. The other instrument parameter settings: microwave power, 1 mW; modulation amplitude, 1 G; scan width, 100 G; sweep time, 40 s. The inset shows the ESR signal of TEMPO.

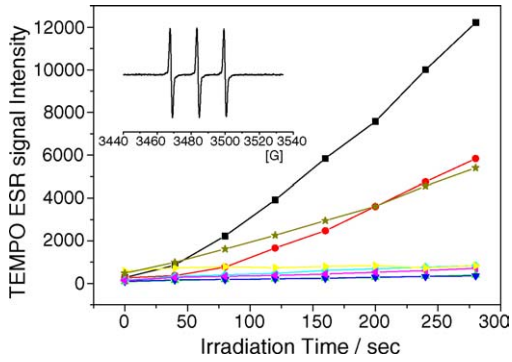

Fig. 5. The dependence of TEMPO signal intensity on the irradiation time in oxygen-saturated DMSO solutions of TEMP (10 μM) and ruthenium complexes or anthracene (O.D. = 0.44 at 355 nm). Ru-2An (■), Ru-lAn (●), anthracence (⋆) Ru-2Py (▲), Ru-lPy (▼), Ru-2Na (♦), Ru-lNa (◄), Ru-0 (►). Instrument parameter settings: microwave power, 1 mW; modulation amplitude, 1 G; scan width, 100 G; sweep time, 40 s; receiver gain, 1×10^5.

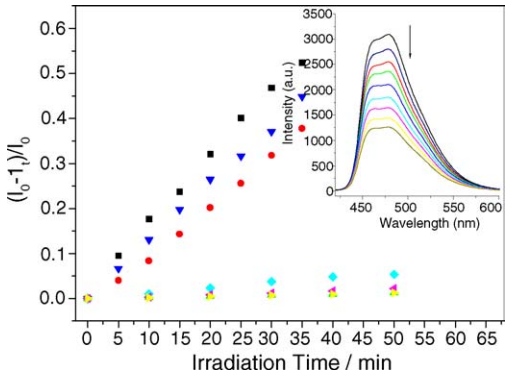

Fig. 6. DPBF consumption percentage as a function of irradiation time in air-equilibrated CH_3OH solution. Ru-2An (■), Ru-lAn (●), $Ru(bpy)_3^{2+}$ (▼), Ru-2Py (♦), Ru-lPy (◄), Ru-2Na (►), Ru-0 (▲). Inset: the emission spectra in the system upon irradiation, the arrow indicates the direction of the changes.

the highly efficient quenching of ^{1}An by ^{1}MLCT state and subsequent transition from ^{3}MLCT state to ^{3}An. In the complex $[Ru(bipy)_2(AnCH_2CH_2bpy)]^{2+}$, it was noted that direct excitation of anthracene localized π–π^* absorption leads to 100% efficient sensitization of MLCT state of the Ru(II) complex; this, in turn, sensitizes the anthracene triplet with unit efficiency[16,32].

Besides TEMP, many organic compounds can react with $^1O_2$, leading to the changes of absorbance and/or fluorescence intensity, and therefore can be utilized to quantitatively measure the $^1O_2$ generation quantum yields of photosensitizers by simply monitoring the UV–vis or fluorescence spectrum. 1,3-Diphenylisobenzofuran (DPBF, Scheme 2) is one of the most reactive with $^1O_2$ [28], with a reported β value of about 10^{-4}. The disappearance of DPBF can be readily followed by measuring the decrease of its fluorescence intensity at emission maximum, and be expressed as a function of photosensitizer's $^1O_2$ generation quantum yield (Φ_Δ) in Eq. (1), where I_{in} is the incident monochromatic light intensity, Φ_{ab} the light absorbing efficiency of the photosensitizer, Φ_r the reaction quantum yield of $^1O_2$ with DPBF, t the irradiation time, I_o and I_t are the fluorescence intensity of DPBF before and after irradiation, respectively. Then, plotting $(I_0 - I_t)$ versus t will give a straight line, and the $^1O_2$ generation quantum yield of the examined photosensitizer can be deduced from the slope ratio as Eq. (2), in which k is the slope and superscript "s" stands for standard:

$$\frac{-\Delta[\mathrm{DPBF}]}{t} = \frac{I_0 - I_t}{t} = I_{in}\Phi_{ab}\Phi_\Delta\Phi_r \quad (1)$$

$$\frac{k}{k^s} = \frac{\Phi_{ab}}{\Phi_{ab}^s} = \frac{\Phi_\Delta}{\Phi_\Delta^s} \quad (2)$$

Fig. 6 shows the plots of $(I_0 - I_t)/I_0$ as the function of irradiation time for Ru(II) bis(terpyridine) complexes. Using $[Ru(II)(bpy)_3]^{2+}$ as standard ($\Phi_\Delta^S = 0.81$ [6]),the Φ_Δ of these complexes were calculated based on Eq. (2) and collected in Table 1. Consisting with the ESR experiments, Ru-2An and Ru-1An distinguish themselves from the other Ru(II) bis(terpyridine) complexes by their extremely high $^1O_2$ generation quantum yield (0.96 and 0.71, respectively), implying their potential application in $^1O_2$-involving processes, such as photocleavage of DNA.

The generation of $^1O_2$ is a bimolecular process, and therefore is dependent on the fraction of donor excited states quenched by O_2. The quenching efficiency (η) can be calculated from Eq. (3):

$$\eta = k_q[O_2]\tau = \left(\frac{1}{\tau} - \frac{1}{\tau_0}\right)\tau \quad (3)$$

where τ_0 and τ are the lifetime of the excited state of the donor in the absence and presence of O_2, respectively ($[O_2]$ is 2.12×10^{-3} M^{-1} air-saturated methanol [37]). Time-resolved absorption measurements gave τ of ^{3}An to be 201 ns for Ru-1An and 193 ns for Ru-2An, so the bimolecular quenching constants k_q of 2.0×10^9 M^{-1} s^{-1} (Ru-1An) and 2.1×10^9 M^{-1} s^{-1} (Ru-2An), and the quenching efficiency η of 0.85 (Ru-1An) and 0.88 (Ru-2An) can be estimated. While the k_q values of 10^9 M^{-1} s^{-1} are typical for quenching of triplet states of organic or inorganic sensitizers by O_2 [6], the lower quenching efficiency than Φ_Δ for Ru-2An is unexpected, because Φ_Δ is related with η by Eq. (4):

$$\Phi_\Delta = \Phi_T \eta f_\Delta^T \quad (4)$$

where Φ_T is the triplet state quantum yield of the sensitizer and f_Δ^T is the fraction of triplet states quenched by O_2 which yield $^1O_2$. The spin-trapping, chemical trapping, as well as flash photolysis mentioned above all indicate Ru-1An and Ru-2An are very efficient in $^1O_2$ generation, or in another word, are very efficiently quenched by O_2 in their excited states. As a result, the residue O_2 in degassed solutions (even by freeze-pump-thaw cycles) may shorten the corresponding τ_0 of ^{3}An, and then yielded a underestimated η. It is obvious that the quenching of ^{3}An for both Ru-1An and Ru-2An is dominated by energy transfer, leading to the efficient

formation of $^1O_2$. Moreover, the ^{3}MLCT with relatively long lifetime may also take effect in $^1O_2$ generation.

3.3. Photodamage of CT-DNA sensitized by Ru(II) bis(terpyridine) complexes

A simple assay for DNA cleavage was applied based on significant enhancement of the fluorescence intensity exhibited by EB upon intercalation into DNA [29–31]. When the concentration of EB is more than two folds that of DNA base pair, the fluorescence intensity of EB is linearly proportional to the concentration of DNA base pair. Any process in which the potential EB binding site was destroyed results in a decrease in fluorescence intensity.

The percentage of binding site remaining at a given time (t) was calculated based on the following equation:

$$\%\text{binding site remaining} = 100 \times \left(1 - \frac{I_0 - I_t}{I_0 - I_{\text{buffer}}}\right) \quad (5)$$

Where I_0, I_t, I_{buf} denote the integrated fluorescence intensities before irradiation, after t min of irradiation, and of DNA-free buffer, respectively.

Ru-2An and Ru-1An were selected to examine their photocleavage capabilities on CT-DNA due to their high $^1O_2$ generation quantum yields, while Ru-2Py and Ru-0 were also studied for comparison.

Upon addition of Ru-2An, Ru-1An, or Ru-2Py into the buffer solutions of EB/CT-DNA, the fluorescence intensity of EB underwent a noticeable decrease (Fig. 7). In contrast, no fluorescence quenching was observed if CT-DNA was not present in the buffer solutions. This fact suggests that the fluorescence quenching may result from the displacement of the intercalating EB from CT-DNA by Ru(II) bis(terpyridine) complexes, in good agreement with the reported result that Ru-2An and Ru-2Py can bind CT-DNA by intercalation of the aryl tail group [10]. The negligible quenching effect of Ru-0 onto the fluorescence of EB/CT-DNA also indicates the presence of aryl groups really enhance the interaction between Ru(II) bis(terpyridine) complexes and DNA. We cannot exclude the possibility that the presence of CT-DNA which is negatively charged reduced the repulsion between both positively charged Ru(II) bis(terpyridine) complexes and EB, and as a result the complexes may quench directly the fluorescence of EB. Provided this mechanism takes effect in fluorescence quenching, it still supports the conclusion that the aryl-substitution favors the interaction of the complexes with CT-DNA.

When the air-saturated buffer solutions of EB/CT-DNA/Ru(II) bis(terpyridine) complex were irradiated with the light above 470 nm, the fluorescence of EB decreased further. According to Eq. (3), the percentage of remaining binding sites of EB onto the damaged CT-DNA was calculated and listed in Table 2. After 20 min of irradiation, 46.6% and 37.2% of the binging sites were damaged for Ru-2An and Ru-1An systems, respectively. In contrast, Ru-2Py and Ru-0 were much less efficient in photodamage of CT-DNA, indicating $^1O_2$ generation plays a key role in photocleavage of CT-DNA sensitized by Ru(II) bis(terpyridine) complexes. The high $^1O_2$ generation quantum yields of Ru-2An and Ru-1An, in combination with their intercalation

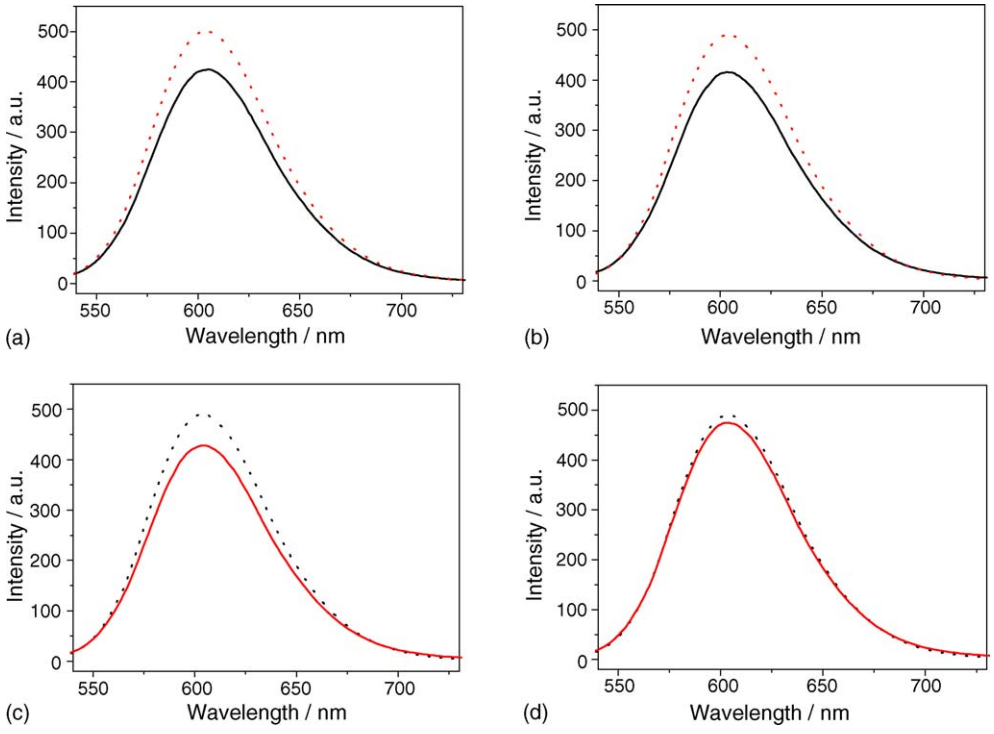

Fig. 7. Emission spectra of EB/CT-DNA buffer solutions in the absence (dot line) and presence (solid line) of Ru-2An (a), Ru-1 An (b), Ru-2Py (c) or Ru-0 (d).

Table 2
Photocleavage of CT-DNA by Ru-2An, Ru-lAn, Ru-2Py or Ru-0 detected by remaining binding site (BSR%) of ethidium bromide to the damaged CT-DNA in an air-saturated ammoniumacetate buffer solution

Sample	Irradiation time (min)				
	4	8	12	16	20
Ru-2An	89.0	79.7	72.9	63.2	53.4
Ru-1An	91.6	83.2	76.7	70.0	62.8
Ru-2Py	97.0	94.3	91.8	88.8	86.2
Ru-0	98.9	98.3	97.9	96.4	95.4

[CT-DNA] = 40 μM, [EB] = 80 μM, [Ru-2An] = 2 μM, [Ru-lAn] = 2.5 μM, [Ru-2Py] = 2 μM, [Ru-0] = 2.5 μM.

and photodamage on CT-DNA, promise their potential application as DNA photocleavers.

4. Conclusion

In this work six Ru(II) bis(terpyridine) complexes functionalized with one or two aryl (including 2-naphthyl, 1-pyrenyl, and 9-anthraceny) groups at 4′-position of terpyridine ligand were studied with focus on their $^1O_2$ generation and DNA-photodamage abilities. It is noted that the triplet excited state of aryl may provide an efficient channel to generate $^1O_2$, and as a result can render the substituted complexes potent photodamage capabilities on DNA if the aryl triplet excited state exists in the complexes as the lowest energy excited state.

Acknowledgment

This work was financially supported by the Ministry of Science and Technology of China (G2000028204).

References

[1] K.E. Erkkila, D.T. Odom, J.K. Barton, Chem. Rev. 99 (1999) 2777–2795.
[2] C. Moucheron, A. Kirsch-De Mesmaeker, J.M. Kelly, J. Photochem. Photobiol. B: Biol. 26 (1994) 165–174.
[3] A.B. Tossi, J.M. Kelly, Photochem. Photobiol. 49 (1989) 545–556.
[4] H.Y. Mei, J.K. Barton, Proc. Natl. Acad. Sci. U.S.A. 85 (1988) 1339–1343.
[5] A. Hergueta-Bravo, M.E. Jiménez-Hernández, F. Montero, E. Oliveros, G. Orellana, J. Phys. Chem. B 106 (2002) 4010–4017.
[6] A.A. Abdel-Shafi, P.D. Beer, R.J. Mortimer, F. Wilkinson, J. Phys. Chem. A 104 (2000) 192–202.
[7] D. Garcia-Fresnadillo, Y. Georgiadou, G. Orellana, A.M. Braun, E. Oliveros, Helv. Chim. Acta 79 (1996) 1222–1238.
[8] Q.G. Mulazzani, H. Sun, M.Z. Hoffman, W.E. Ford, M.A.J. Rodgers, J. Phys. Chem. 98 (1994) 1145–1150.
[9] J.-P. Sauvage, J.-P. Collin, J.-C. Chambron, S. Guillerez, C. Coudret, V. Balzani, F. Barigelletti, L. De Cola, L. Flamigni, Chem. Rev. 94 (1994) 993–1019.
[10] K.K. Patel, E.A. Plummer, M. Darwish, A. Rodger, M.J. Hannon, J. Inorg. Biochem. 91 (2002) 220–229.
[11] S. Encinas, L. Flamigni, F. Barigelletti, E.C. Constable, C.E. Housecroft, E.R. Schofield, E. Figgemeier, D. Fenske, M. Neuburger, J.G. Vos, M. Zehnder, Chem. Eur. J. 8 (2002) 137–150.
[12] V. Grosshenny, A. Harriman, R. Ziessel, Angew. Chem. Int. Ed. Engl. 34 (1995) 2705–2708.
[13] V. Balzani, A. Juris, M. Venturi, S. Campagna, S. Serroni, Chem. Rev. 96 (1996) 759–833.
[14] M. Maestri, N. Armaroli, V. Balzani, E.C. Constable, A.M.W. Cargill Thompson, Inorg. Chem. 34 (1995) 2759–2767.
[15] A. El-ghayoury, A. Harriman, A. Khatyr, R. Ziessel, Angew. Chem. Int. Ed. 39 (2000) 185–189.
[16] X. Wang, A.D. Guerzo, R.H. Schmehl, J. Photochem. Photobiol. C: Photochem. Rev. 5 (2004) 55–77.
[17] A.F. Morales, G. Accorsi, N. Armaroli, F. Barigelletti, S.J.A. Pope, M.D. Ward, Inorg. Chem. 41 (2002) 6711–6719.
[18] R. Passalacqua, F. Loiseau, S. Campagna, Y.Q. Fang, G.S. Hanan, Angew. Chem. Int. Ed. 42 (2003) 1608–1611.
[19] A. Harriman, M. Hissler, A. Khatyr, R. Ziessel, Chem. Commun. (1999) 735–736.
[20] M. Hissler, A. Harriman, A. Khatyr, R. Ziessel, Chem. Eur. J. 5 (1999) 3366–3381.
[21] D.S. Tyson, K.B. Henbest, J. Bialecki, F.N. Castellano, J. Phys. Chem. A 105 (2001) 8154–8161.
[22] G. Albano, V. Balzani, E.C. Constable, M. Maestri, D.R. Smith, Inorg. Chim. Acta 277 (1998) 225–231.
[23] W.L.F. Armarego, C.L.L. Chai, Purification of Laboratory Chemicals, 5th ed., Elsevier Science, London, 2003.
[24] Friitz, Krohnke, Synthesis (1976) 1–24;
A. Gulyani, R. Srinivasa Gopalan, G.U. Kulkarni, S. Bhattacharya, J. Mol. Struct. 616 (2002) 103–112.
[25] E.C. Constable, C.E. Housecroft, M. Cattalini, D. Phillips, New J. Chem. 2 (1998) 193–200.
[26] N.H. Damrauer, T.R. Boussie, M. Devenney, J. Am. Chem. Soc. 119 (1997) 8253–8268.
[27] I.P. Evans, A. Spencer, G. Wilkinson, J. Chem. Soc., Dalton Trans. (1973) 204–209.
[28] R.H. Young, K. Wehrly, R.L. Martin, J. Am. Chem. Soc. 93 (1971) 5774–5779.
[29] W.A. Pruetz, Radiat. Environ. Biophys. 23 (1984) 1–6.
[30] W.A. Pruetz, Radiat. Environ. Biophys. 23 (1984) 7–18.
[31] H.C. Birnboim, J.J. Jevcak, Cancer Res. 41 (1981) 1889–1892.
[32] G.J. Wilson, A. Launikonis, W.H.F. Sasse, A.W.-H. Mau, J. Phys. Chem. A 101 (1991) 4860–4866.
[33] B. Maubert, N.D. McClenaghan, M.T. Indelli, S. Campagna, J. Phys. Chem. A 107 (2003) 447–455.
[34] D.B. MacQueen, J.R. Eyler, K.S. Schanze, J. Am. Chem. Soc. 111 (1989) 7448–7454.
[35] (a) Y. Lion, M. Delmelle, A.V. Vorst, Nature 263 (1976) 442–445;
(b) C. Hadjur, A. Jeunet, P. Jardon, J. Photochem. Photobiol. B: Biol. 26 (1994) 67–74.
[36] G. Rossbroich, N.A. Garcia, S.E. Braslavsky, J. Photochem. 31 (1985) 37–47.
[37] S.L. Murov, I. Carmichael, G.L. Hug, Handbook of Photochemistry, Marcel Dekker, New York, 1973.